ELSEVIER

Thermochimica Acta 374 (2001) 105–114

thermochimica acta

www.elsevier.com/locate/tca

Bitumen microstructure by modulated differential scanning calorimetry

J-F. Masson*, G.M. Polomark

Institute for Research in Construction, National Research Council of Canada, Ottawa, ON, Canada K1A OR6

Received 18 August 2000; received in revised form 2 February 2001; accepted 3 February 2001

Abstract

Bitumen was analysed by modulated differential scanning calorimetry (MDSC). This method allows for the deconvolution of overlapping reversing and non-reversing thermal events and it allows for the observation of transitions not visible on the thermal curve obtained by standard DSC. The reversing thermal curve revealed two glass transition temperatures (T_g) in bitumen. One transition, at -20°C, was assigned to the maltenes, the other at 70°C to the asphaltenes. The heat capacity of these transitions was found to depend on thermal history. From the total heat capacity, it was calculated that the relative size of the bitumen repeat unit is between 36 and 91 g mol^{-1}, which given an average molecular weight of 300–1000 g mol^{-1} for bitumen, translates into a ''degree of polymerisation'' of $\sim$10. After cooling from the melt and annealing at 22°C, bitumen microstructure was found to develop in three stages. Most rapid is an ordering process that occurs when bitumen is quenched from the melt. It is postulated that this first stage arises from the partial ordering of simple aromatic structures into micro- and nano-phases; a second stage, which ends within $\sim$3 h of annealing, relates to the ordering of somewhat larger aromatic structures; and a third stage, which ends in $\sim$16 h, is thought to arise from the ordering of the largest bitumen structures, the resins and the asphaltenes. The development of bitumen microstructure and the calculations of the entropy and enthalpy of transitions suggest that bitumen is a multi-phase system with a small crystalline phase, and a large mesophase, i.e. a structured amorphous phase. Published by Elsevier Science B.V.

Keywords: Bitumen; Transitions; Heat capacity; Ordering; Calorimetry; Microstructure

1. Introduction

Bitumen is a natural polymer of low molecular weight, and like all polymers it is viscoelastic [1]. At low temperatures it is rigid and brittle, at room temperature it is flexible, and at higher temperatures it flows. In contrast to synthetic polymers, however, bitumen viscoelastic behaviour is poorly related to microstructure. In synthetic polymers, a flexible and apolar backbone leads to a low glass transition temperatures (T_g), whereas high molecular weight, cross-linking, interchain interactions, and crystallinity enhance high temperature behaviour [2,3]. The correlation between structure and property of synthetic polymers is so well defined that the latter can be predicted with relatively few relationships [4].

In contrast, the factors that govern the viscoelasticity of bitumen are not well-defined, primarily because a precise molecular structure and repeat unit for bitumen is not established. The chemistry of bitumen is most often defined in terms of fractions obtained by chromatography [5,6], e.g. saturates,

* Corresponding author. Tel.: +1-613-993-2144; fax: +1-613-954-5984.
E-mail address: jean-francois.masson@nrc.ca (J-F. Masson).

0040-6031/01/$ – see front matter. Published by Elsevier Science B.V.
PII: S0040-6031(01)00478-6

resins, aromatics and asphaltenes fractions (SARAs), or in terms of maltenes and asphaltenes content, the maltenes being the de-asphaltenated portion of bitumen. Each SARAs fraction is a mixture with a complexity, aromaticity, heteroatom content, and molecular weight that increase in the order S < A < R < As [6]. As a result of this continuum in bitumen composition, the viscoelastic curve for bitumen is rather uneventful as it shows a smooth change in modulus with temperature [7].

Due to the rather uninformative rheological curve of bitumen, much work in the last decade has been performed with differential scanning calorimetry (DSC) to study bitumen microstructure and its relation to physical properties [8–14]. The DSC curve reveals a T_g and two endotherms (Fig. 1). Claudy et al. [9,10] have related T_g to the saturates and aromatics and the endotherms to the saturates, while Harrison et al. [8] have related the endotherms to fractions other than the saturates.

In this paper, we use modulated DSC (MDSC) to investigate the thermal behaviour of bitumen. This relatively new and powerful method was developed by Reading et al. [15,16], who described its mathematical basis extensively [17,18]. The method has been applied to the study of the glass transition and the melting of polymers, liquid crystals and hydrocarbons [19]. It provides greater sensitivity than regular DSC as it allows for differentiating between reversing and non-reversing thermal behaviours in materials (Fig. 2). Reversing events include those that can be brought to equilibrium during the period of a modulated temperature signal used in the MDSC experiment. Most important in this respect are the atomic motions responsible for the heat capacity [20]. As a result, the latter is the major contributor to the reversing curve. Effects that cannot be modulated and brought to equilibrium are excluded from the reversing curve and show as non-reversing, e.g. oxidation, evaporation, decomposition, relaxation, reaction [15,16].

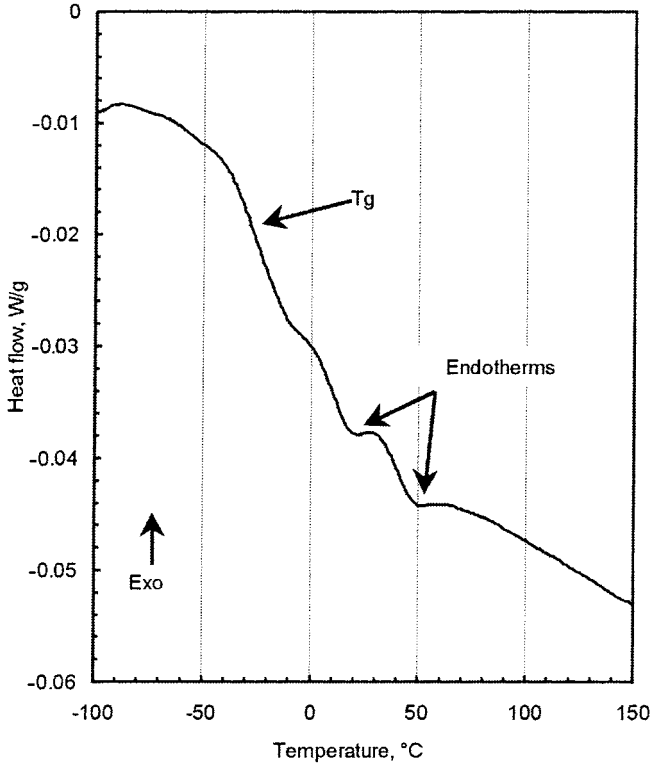

Fig. 1. Typical DSC curve for bitumen.

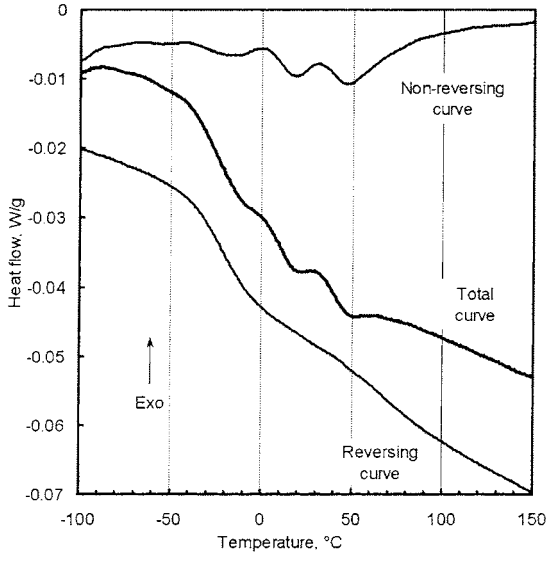

Fig. 2. Total, reversing and non-reversing heat-flow curves for bitumen.

Interestingly, the melting of crystals can include both reversing and non-reversing contributions [19,21].

This work shows that MDSC can provide new information on the structure and thermal behaviour of bitumen. The technique allows for the fractionation of thermal events without the physical fractionation of bitumen itself. The work also shows that the thermal profile of bitumen is time dependent and that it develops in three stages, each of which can be related to a distinct bitume structure. The results provide evidence for a mesophase structure in bitumen, much like that encountered in liquid crystals.

2. Experimental

Bitumen was provided by Petro-Canada. It had a 85/100 penetration grade and a respective saturates, aromatics, resins, and asphaltenes content of 3, 33, 34, and 30%, as measured with the Iatroscan by successive elution in heptane, toluene and tetrahydrofuran. Details of the method are provided elsewhere [22]. The as-received bitumen was stored several months at 22°C before being analysed.

All experiments were carried out with a TA instrument 2100 MDSC. The sample was purged with helium at a rate of 50 ml/min and liquid nitrogen was used for cooling. Sealed pans were used to encapsulate about 25 mg of sample. For accurate heat capacity measurements, the sample and reference pans were matched. The heat capacity was calibrated with sapphire, whereas temperature and baseline were calibrated with indium. In modulated heating and cooling experiments, an oscillation period of 60 s and amplitude of ±0.47°C were used.

Quenching, as defined here, was the cooling of the sample at the maximum permissible rate by the calorimeter, an average of about 20°C min^{-1} down to −100°C. Annealing as defined here is the storage at 22°C (room temperature) for a specified time.

Bitumen was subjected to three successive thermal regimes: (a) quenching of as-received bitumen from 22 to −100°C followed by heating at 3°C min^{-1} to 150°C; (b) quenching to 22°C, and annealing for 0, 1, 2, 3, 16, 24 h; (c) quenching to −100°C and heating again to 150°C. At the beginning and end of each heating and cooling run, bitumen was held isothermally for 5 min. Reproducibility and absence of oxidation was verified by comparing cooling and heating reversing curves. In this case, bitumen was cooled from 150 to −100°C at 3°C min^{-1} and heated again, at the same rate, to 150°C.

2.1. Data analysis

The recording, analysis and deconvolution of the signals were done with the TA software for the MDSC. Reported curves were smoothed by use of the least square method. Little smoothing was applied to the non-reversing curves and relatively more smoothing was applied to derivative curves, which are inherently noisy. The level of smoothing was selected to give minimum distortion and no shift of peaks. In all figures, the exotherm points upwards. The heat capacities reported are those obtained from the peak areas of the derivative curves as described elsewhere [23].

3. Results

3.1. Conventional and modulated DSC

Preliminary analysis consisted in obtaining a DSC thermal curve of the as-received bitumen (Fig. 1). The signal is that of a bitumen cooled from the melt and

annealed at room temperature for several months. Based on a common interpretation [9,10], there would be a glass transition temperature (T_g) centred around −20°C, followed by two endotherms at ∼20 and ∼50°C for the melting of saturates.

Fig. 2 shows how the regular DSC trace is deconvoluted by MDSC into reversing and non-reversing components. The non-reversing component contributes the least to the total heat flow and only adds details to the overall thermal profile. For this reason, the thermal events below 0°C in the non-reversing curve are invisible in the total heat flow curve. The reversing component is the largest contributor the total heat flow. It shows a large decrease between −50 and 0°C and a much smaller one between 0 and 150°C. Interestingly, this small decrease of the reversing curve remains hidden in the total heat flow curve.

3.2. Time-dependence of the reversing and non-reversing profiles

After quenching from 150°C, bitumen was annealed for various times at 22°C and reheated. Fig. 3 shows the excellent reproducibility in reversing heat flow between the heating and cooling curves in the range −100 to 150°C. The overlap of the curves indicate that bitumen remains unoxidized during the heat treatment. It is also noted that the reversing heat flow curve contains no endothermic contribution that can be attributed to reversible melting of a crystalline phase as observed in semi-crystalline polymers [19,21]. This would be consistent with the predominantly amorphous nature of bitumen.

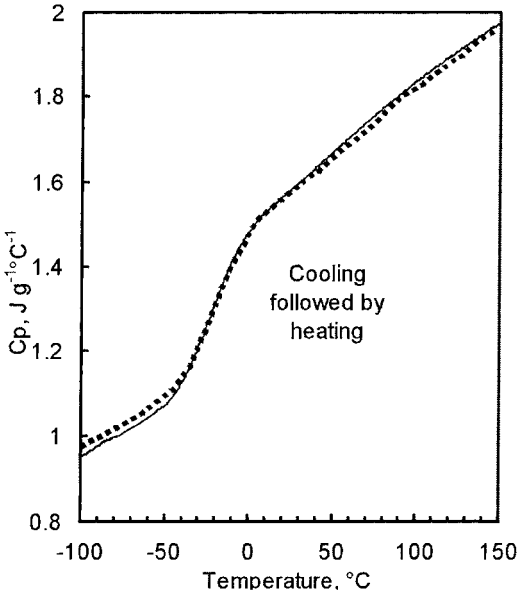

Fig. 3. Reproducibility of the heat capacity upon heating and cooling.

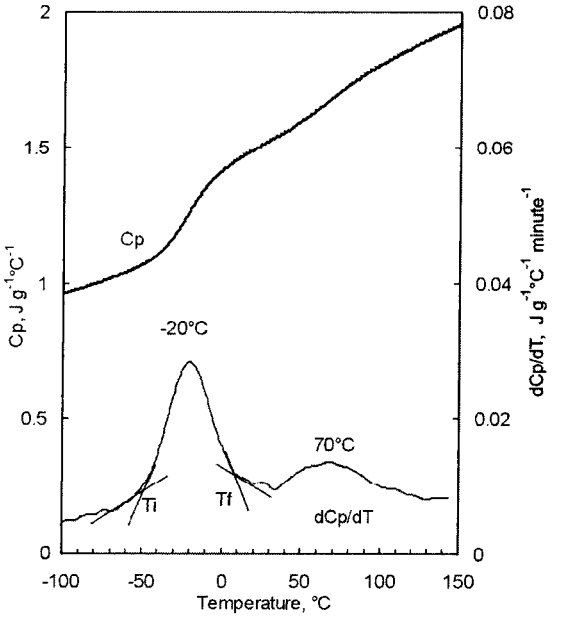

Fig. 4. Heat capacity and its derivative for the as-received bitumen.

The reversing heat flow, Q, can be converted to heat capacity, C_p, by dividing by the underlying heating rate [15,16]. At T_g, the change in heat capacity is defined by its derivative as $\Delta C_p = \int (\mathrm{d}C_p/\mathrm{d}T)\,\mathrm{d}T$ [23]. Fig. 4 shows that the as-received bitumen had two transitions, a large T_g at −20°C, and a small and broad T_g centred at 70°C. These transitions, with respective heat capacities of 0.22 and 0.06 J g^{-1}, were effected by thermal history.

After bitumen was heated to 150°C and cooled, it was annealed for various times. The effect of annealing time on the T_g's is shown in Fig. 5. The T_g at 70°C is almost absent when bitumen is not annealed, but it is fully developed in the as-received bitumen, which was stored several months at 22°C. The ΔC_p at −20°C shows the reverse trend, it is largest without annealing and lowest in the as-received sample. In no case was there a shift in the T_g's from −20 or 70°C, but a

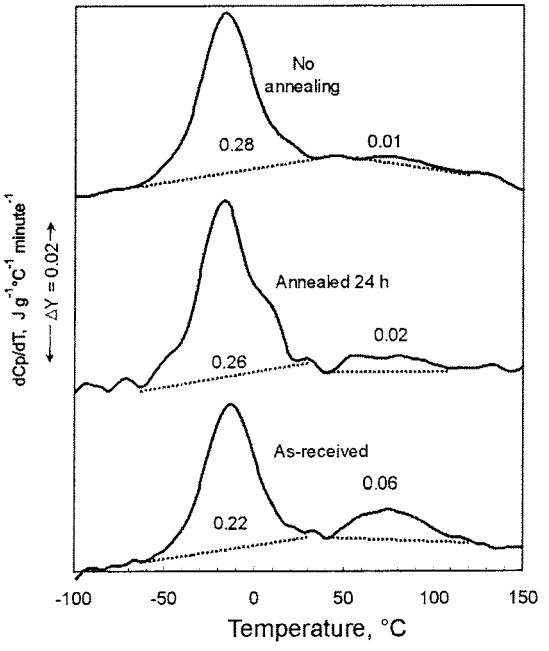

Fig. 5. Heat capacity of bitumen after annealing for various times. The numbers indicate the heat capacity (in $J\,g^{-1}\,°C^{-1}$) of the various peaks.

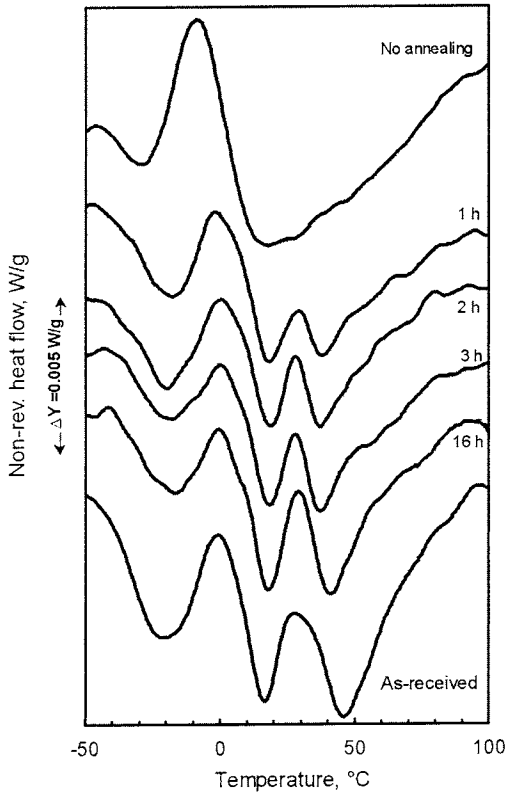

Fig. 6. Change in the profile of the non-reversing curve for bitumen annealed for various times.

shoulder appeared at 10°C after 24 h of annealing. Regardless of annealing time, the change in C_p between −100 and 150°C increased by 1.0 $J\,g^{-1}\,K^{-1}$ (Fig. 4) whereas the sum of ΔC_p at the T_g's remained at ∼0.3 $J\,g^{-1}$ (Fig. 5).

The non-reversing behaviour of bitumen was also affected by annealing. Without annealing, the curve was very simple (top of Fig. 6). It showed an exotherm at −10°C, above a baseline drawn straight from −50 to 100°C, and what would appear to be two endotherms, one at −31°C and another at 20°C. After annealing, all curves showed what seemed to be three endotherms centred at −20, 20, and 40−50°C.

4. Discussion

4.1. Heat capacity

The dC_p/dT curve (Fig. 4) shows two peaks at temperatures where the heat flow rate increases most rapidly. These peaks correspond to glass transition temperatures that arise from amorphous phases [2]. The presence of two T_g's indicate the presence of at least two disordered phases in bitumen. More phases could exist, however, because T_g's can overlap. The shoulder in the middle curve of Fig. 5 may be an example of such an overlap.

The multiple T_g's in bitumen open a window on its microstructure as T_g relates to the composition and structure of the phase from which it originates. The extraordinary breath of the transitions, over 50°C for each T_g, is consistent with a multicomponent and complex phase structure. Given that molecules with polar or bulky groups show higher T_g's than molecules with flexible chains of apolar repeat units [2], and the increase in complexity and rigidity of bitumen fractions in the order of S < A < R < As, we expect their T_g's to show the same order. Claudy et al. [9,10] have shown by DSC that the saturates of bitumen have lower T_g's than the aromatics (−60 and −20°C, respectively), but the T_g of the resins and the asphaltenes have remained elusive.

A simple geometric progression would place the respective T_g's of the resins and asphaltenes at 20 and 60°C, and that of the maltenes at −20°C. This is obviously an over simplistic treatment of the glass transition of bitumen, but it provides a trend, which coupled with the expected increase in T_g with polarity, stiffness, and molecular weight, is consistent with a T_g at −20°C for the maltenes and a T_g at 70°C for the asphaltenes, as observed in Fig. 4. The relative ease with which the asphaltenes can be precipitated out of bitumen with some solvent [6] also supports a bi-phasic system. These phases can be observed independently here only because of the sensitivity and the deconvolution power of MDSC over DSC.

The presence of two T_g's in bitumen is an indication of phase segragation. The change in the T_g's over time (Fig. 5) also provides an indication of the size of the domains from which the T_g's originate. When two intermixed phases show domain sizes exceeding 15–20 nm, two T_g's are observed, and when the domain size is smaller there is a shift in the T_g's or a blending of the T_g's into one [24–26]. The change in the T_g at 70°C would thus suggest that the maltenic and asphaltenic phases in as-received bitumen are larger than 15–20 nm, but that they are of a lesser size in unannealed bitumen. In other words, after bitumen is heated to its liquid state and quenched, the resulting mixture is a solid solution of asphaltenes in maltenes that segregate over time. This has important implications for domain size measurements by X-ray diffraction on which bitumen microstructure models are based [27], and it implies that thermal history of the sample must be rigorously the same when two methods are compared, e.g. NMR and DSC [28].

It is noteworthy that with the blending of the asphaltenes and maltenes obtained from melting (top of Fig. 5), the T_g's would be expected to move closer together, yet they remain stationary. This violation of the rule of mixtures might be typical of bitumen, as it is also inferred from other work on the T_g of bitumen and that of its saturates and aromatics fractions [9,10]. This seemingly anomalous behaviour may be explained by the formation of an interphase (a third phase) with its own T_g. The formation of an interphase, with a composition and T_g that change with annealing time, would be consistent with the appearance of a shoulder at 10°C in the middle curve of Fig. 5, and with the change in ΔC_p at −20 and 70°C. When the interphase is maltene-rich, it overlaps with the former transition, and when it is asphaltene-rich, it overlaps with the latter. More MDSC work on the T_g of bitumen and its fractions obtained by flash chromatography [22] will be published later.

The ΔC_p at T_g provides other information on the structure of bitumen. For amorphous organic materials like polymers and liquid crystals, ΔC_p at T_g is typically 11 J K^{-1} mol^{-1} for a mole of mobile repeat unit [20,29]. The repeat unit of bitumen being undefined, its ΔC_p is measured on a weight basis, i.e. in J K^{-1} g^{-1} rather than in J K^{-1} mol^{-1}. The ratio of ΔC_p for organic materials (in J K^{-1} mol^{-1}) to ΔC_p for unannealed bitumen at −20°C (in J K^{-1} g^{-1}) allows an estimation of the relative size of the bitumen flexible repeat unit: 11 J K^{-1} mol^{-1} to 0.3 J K^{-1} g^{-1} = 36 g mol^{-1}. This value indicates that the average bitumen molecule, with an average molecular weight of 300–1000 g mol^{-1} [30,31] cannot be considered as the repeat unit for bitumen. With a value of 36 g mol^{-1}, the average repeat unit for bitumen can be represented by a structure such as –$(CH_2CH_2OCH_2CH_2)_{0.5}$–. The heat capacity of bitumen can be as low as 0.12 J K^{-1} g^{-1} [9,10], however, so the size of the bitumen flexible repeat unit can be as large as 91 g mol^{-1}, which can be represented by an aromatic structure such as $C_6H_5CH_2$–. The ratio of the typical average molecular weight for bitumen and the repeat unit indicates that the average ''degree of polymerisation'' of bitumen is ∼10.

4.2. Time-dependence of non-reversing curve

When bitumen his heated above the melt temperature and then cooled to 22°C, the resulting profile of the non-reversing curve depends on annealing time at 22°C (Fig. 6). Hence bitumen is not in a stable solid amorphous state when it is cooled but in a metastable state. In other words, the kinetic bitumen phase obtained upon cooling tends towards a more stable thermodynamic state over time. Such temperature-time-transformation [32], common in minerals and metals was recently shown to occur in blends of solid hydrocarbons [33]. The time for transformation of bitumen into a stable phase takes at least 16 h as shown in Fig. 6, but the reversing curves for the as-received bitumen (Fig. 5) suggest that it takes several weeks to attain equilibrium.

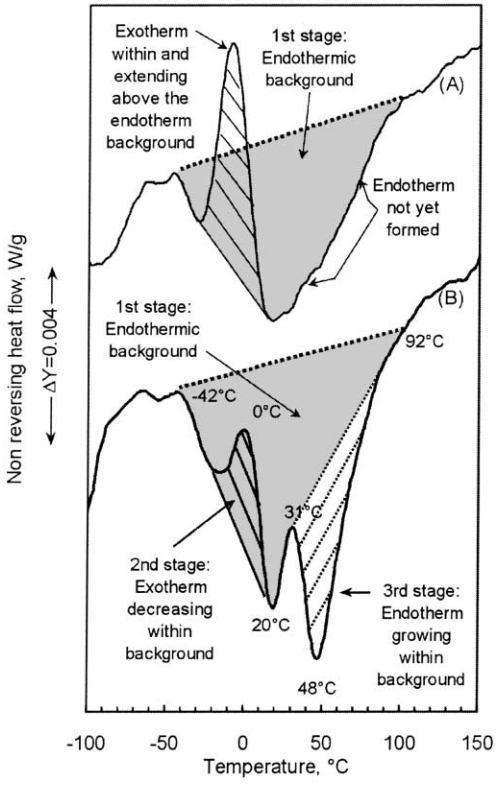

Fig. 7. Breakdown of the three overlapping thermal events in the non-reversing curve of bitumen.

Bitumen metastability may arise from several factors. The microscopic observations of Claudy et al. [11,12] on bitumen stored 24 h at 25°C suggest that crystallisation of saturates is responsible for metastability. In contrast, at temperatures close to T_g, the loss of free volume may be a governing factor [34], which implies a densification of the amorphous region of bitumen. The results shown here suggest that the ordering of aromatic structures also contributes to metastability and densification.

Bitumen metastability is governed by three overlapping thermal events (Fig. 7). The first event produces a background, an endothermic envelope that, in the bitumen studied, begins at −42°C and ends at 92°C. The immediate appearance of this background upon cooling indicates that it arises from mobile segments that can order on a very short scale. The centre and minimum temperature of this background remains unchanged at ∼20°C regardless of thermal history (Figs. 6 and 7).

The second thermal event is the exotherm that centres at ∼0°C and which overlap with the background (Fig. 7a). The exotherm, most easily seen in a second heating run immediately after cooling from 150°C when it rises above the baseline (Fig. 7a), stems from materials that organize upon heating and which melt at higher temperatures. Upon annealing, the exotherm is reduced due to self-ordering, as observed by a decrease in the exotherm (Fig. 6). After 3 h, there is little change in the exotherm as it stabilizes below the baseline. In regular DSC an exotherm is only rarely identified because it is most often shadowed by T_g [13]. Here we have the first indication that the exotherm is present below the baseline regardless of thermal history (Fig. 7b). The exothermic ordering should also not be confused with relaxation, which is endothermic and which occurs in the amorphous phase. A detailed account of the effect of annealing temperature on the exotherm is forthcoming.

The third thermal event is an endotherm between 40 and 50°C that overlaps with the higher temperature side of the endothermic background (Fig. 7b). The small endotherm grows regularly upon annealing (Fig. 6). Based on the analysis of the exotherm at ∼0°C, the profile between 20 and 70°C could easily be mistaken to also include an exotherm that centres at 31°C (Fig. 8). However, an exotherm would be of maximum intensity immediately after quenching, like the exotherm at 0°C, which it is not. The thermal event between 30 and 90°C is therefore an endotherm. The size of this endotherm is time dependent. It grows very slowly over several months but the greatest development occurs in less than 24 h (Fig. 9).

4.3. Origin of thermal events

The time dependent behaviour of bitumen shown in the non-reversing curve stems from the overlap of rapid, medium (3 h) or slow (16–24 h) thermal events. Each event may be associated with a specific bitumen sub-structure or phase. Most rapid is an immediate ordering process that occurs when bitumen is quenched from the melt, and which gives rise to the background in Fig. 7. This process most likely arises from small scale molecular ordering, and given the breadth of the transition (130°C), these motions probably arise within micro- and nano-phases that broaden transitions due to surface effects [25,25].

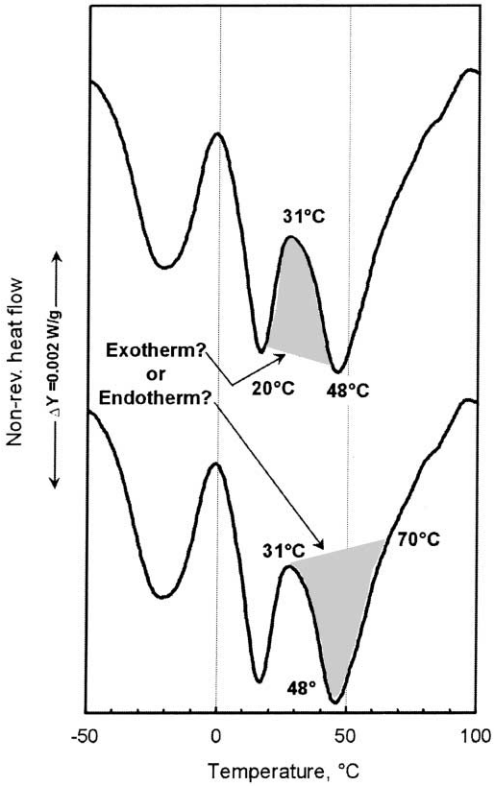

Fig. 8. Non-reversing curve for fully annealed bitumen. The observation of a single curve does not allow for distinguising between an exotherm or an endotherm between 20 and 70°C. See text for details.

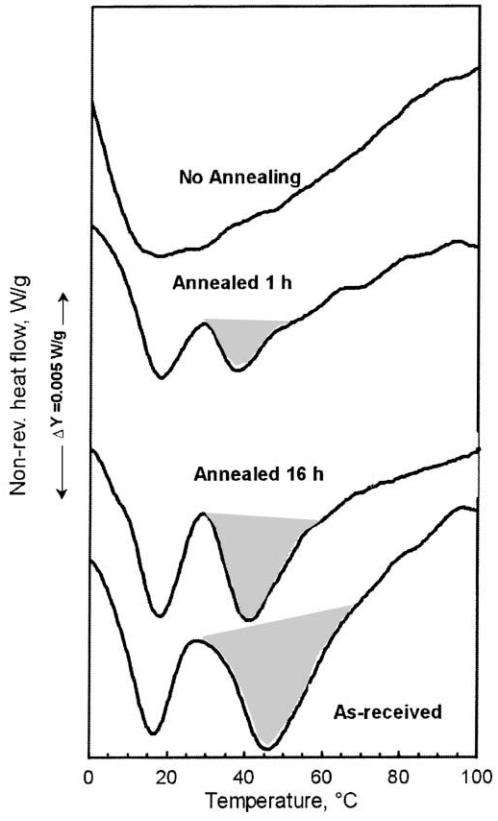

Fig. 9. Enlargement of the non-reversing curve between 0 and 100°C. The shaded area helps to view the growth of an endotherm at 40–50°C.

Upon heating, the disordering of these phases give rise to the endothermic background. The broad endotherm may partly arise from the crystallisation of saturates, as it has been suggested [9–14], but as will be shown shortly with the calculation of the entropy of transition, it most likely arises from the ordering of simple aromatic structures such as those known to occur in liquid crystalline mesophases [35].

The second thermal event arises from slower dynamics and it is completed in ∼3 h. After quenching to, and annealing at, 22°C bitumen self-orders on standing. The extend of this ordering is inversely proportional to the height of the exotherm at 0°C, and it is at maximum in the absence of annealing. Recalling the inverse relationship between diffusion rate and molecular size, this ordering may arise from the diffusion and assembly of structures larger than those responsible for the background, e.g. naphtalene-like aromatics. Again, it may arise from the twisting and alignment of aromatic centres along an order axis to produce a mesophase.

The third and slowest thermal event is the growing of an endotherm over 16–24 h at 40–50°C. Given the slow rate of ordering, the transition may arise from the slow diffusion of relatively large and high molecular weight structures to form independent domains. Resins and asphaltenes, multi-rings and multi-arm structures, may be major contributors to this transition. Evidence for this assignments is forthcoming [36].

A mesophase structure for bitumen is consistent with the entropy of transition, $\Delta S = \Delta H/T$, obtained from the background (Fig. 7). Considering an average molecular weight of 1000 g mol^{-1} for bitumen [27,28], a transition centre at $T = 300$ K and $\Delta H \approx 7$ J g^{-1}, the calculated entropy of transition is

$\sim$23 J K^{-1} mol^{-1}. This value is typical of that for the orientational disordering of *irregular* structures [20,25,26]. This implies that the major contributor to the background could be an ensemble of alkylated aromatics of various sizes and shapes, and that the transition arises from isotropisation, a situation most common in mesophases [20,25,26]. The disordering of more regular structures, i.e. melting of the saturates, may then only be a small contributor to the endotherm. This is consistent with the work of Harrison et al. [8] who failed to find a correlation between saturates content and the size of the endotherm. This is also shown by a simple calculation. The heat of fusion of the saturates is 17–30 J g^{-1} [9,10,34]. With a 3% saturates content for the bitumen at hand, the expected heat of fusion was 0.5–1.0 J g^{-1}. Yet that obtained was $\sim$7 J g^{-1}, which indicates that more than 85% of the background arises from isotropization of fractions other than the saturates.

5. Conclusion

Bitumen has been analysed by means of modulated differential scanning calorimetry (MDSC). The technique allows for the deconvolution of reversing and non-reversing thermal events into two thermal curves that allow for the observation of thermal transitions not visible on the single thermal curve obtained by standard DSC. The reversing thermal curve, related to ΔC_p reveals two glass transition temperatures (T_g) in bitumen annealed several months: a transition at -20°C is assigned to the maltenes and another at 70°C to the asphaltenes. From the total ΔC_p at the T_g's, it is calculated that the relative size of the bitumen repeat unit is between 36 and 91 g mol^{-1}, which can be represented by segments such as $-(CH_2CH_2OCH_2CH_2)_{0.5}-$ and $C_6H_5-CH_2-$, respectively. From the size of these repeat units and the average molecular weight for bitumen, the average "degree of polymerisation" for bitumen is estimated at $\sim$10. Hence bitumen is not a polymer as often suggested, but an oligomer.

The non-reversing thermal curve showed two endotherms and one exotherm. The entropy of the combined endotherms, ΔS, was calculated to be $\sim$23 J K^{-1} mol^{-1}, which corresponds to the disordering of irregular structures. This implies that an ensemble of substituted aromatics of various sizes and shapes is a major contributor to the endotherms. From the enthalpy of the endotherms, ΔH, it is estimated that $\sim$85% of the total endotherm arises from isotropisation of these aromatics, whereas only $\sim$15% arises from the melting of the partly crystalline saturates. Taken together, ΔS and ΔH indicate that bitumen is a multi-phase system with a small crystalline phase and a large mesophase, i.e. a structured amorphous phase.

The thermal events in the non-reversing thermal curve were found to be time dependant. This time dependence allowed for the identification of the likely origin of theses transitions, which interestingly develop in stages. A rapid first stage produces a broad endothermic background that develops upon cooling bitumen from the melt. It possibly arises from the ordering of simple aromatic structures into micro- and nano-phases. A second stage is visible by the decrease over 3 h of an exotherm at 0°C. The exotherm, is thought to relate to the ordering of more complex aromatics into a mesophase. The third stage involves the development of a secondary endotherm within the large endothermic background. It is centred at 40–50°C and it matures mostly within 24 h. This endotherm likely stems from the ordering of large multi-ring and multi-arm bitumen structures, e.g. resins and asphaltenes, also into a mesophase.

Finally, in working with bitumen it is customary to wait at least 24 h before proceeding with an analysis so that reproducibility is maintained. This work shows, however, that there is much value in not waiting so long to proceed with analysis, provided that thermal history is controlled. It is then possible to get better insight into the structure of bitumen and learn how it develops in different conditions. This may lead to a better understanding of bitumen microstructure and how it affects its properties.

References

[1] C.Y. Cheung, D. Cebon, J. Mat. Civ. Eng. 9 (3) (1997) 117.
[2] A. Eisenberg, The Glassy State and the Glass Transition, in Physical Properties of Polymers, 2nd Edition, American Chemical Society, Washington, DC, 1993, p. 61.
[3] J. Ferry, Viscoelastic Properties of Polymers, 3rd Edition, Wiley, New York, 1980.
[4] D.W. van Krevelen, Properties of Polymers: Their Correlation with Chemical Structure, Their Numerical Estimation and Prediction from Additive Group Contributions, 3rd Edition, Elsevier, New York, 1990.

[5] J.L. Goodrich, J.E. Goodrich, W.J. Kari, Transp. Res. Rec. 1096 (1986) 146.
[6] J.G. Speight, The Chemistry and Technology of Petroleum, 3rd Edition, Marcel Dekker, New York, 1999.
[7] J.L. Goodrich, Proc. Assoc. Asphalt Paving Technol. 57 (1988) 116.
[8] I.R. Harrison, G. Wang, T.C. Hsu, A Differential Scanning Calorimetry Study of Asphalt Binders, Report SHRP-A/URF-92-612, Strategic Highway Research Program, National Research Council, Washington, DC, 1992.
[9] P. Claudy, J.-M. Létoffé, G.N. King, B. Brûlé, J.-P. Planche, Bull. Liaison Labo. P. et Ch. 165 (1990) 85.
[10] P. Claudy, J.-M. Létoffé, G.N. King, B. Brûlé, J.-P. Planche, Fuel Sci. Tech. Int. 9 (1) (1991) 71.
[11] P. Claudy, J.-M. Létoffé, G.N. King, J.-P. Planche, Liaison Labo. P. et Ch. 177 (1992) 45.
[12] P. Claudy, J.-M. Létoffé, G.N. King, J.-P. Planche, Fuel Sci. Tech. Int. 10 (4-6) (1992) 735.
[13] P. Claudy, J.-P. Létoffé, D. Martin, J.-P. Planche, Thermochim. Acta 324 (1998) 203.
[14] J.-P. Planche, P. Claudy, J.-M. Létoffé, D. Martin, Thermochim. Acta 324 (1998) 223.
[15] M. Reading, Trends Polym. Sci. 1 (8) (1993) 248–253.
[16] P.S. Gill, S.R. Sauerbrunn, M. Reading, J. Therm. Anal. 40 (1993) 931.
[17] K.J. Jones, I. Kinshott, M. Reading, A.A. Lacey, C. Nikopoulos, H.M. Pollock, Themochim. Acta 304/305 (1997) 187.
[18] A.A. Lacey, C. Nikopoulos, M. Reading, J. Therm. Anal. 50 (1997) 279.
[19] B. Wunderlich, A. Boller, I. Okazaki, K. Ishikiriyama, W. Chen, M. Pyda, J. Pak, I. Moon, R. Androsch, Thermochim. Acta 330 (1999) 21.
[20] B. Wunderlich, Thermochim. Acta 340/341 (1999) 37.
[21] B. Wunderlich, I. Okazaki, K. Ishikiriyama, A. Boller, Thermochim. Acta 324 (1998) 77.
[22] L. Raki, J-F. Collins, P. Masson, Energy Fuels 14 (2000) 160.
[23] D.J. Hourston, M. Song, A. Hammiche, H.M. Pollock, M. Reading, Polymer 38 (1) (1997) 1.
[24] D. S Kaplan, J. Appl. Polym. Sci. 20 (1976) 2615.
[25] D.J. Hourston, F.-U. Schafer, J.S. Bates, M.H.S. Gradwell, Polymer 39 (15) (1998) 3311.
[26] D.J. Hourston, F.-U. Schafer, M.H.S. Gradwell, M. Song, Polymer 39 (23) (1998) 5609.
[27] T.F. Yen, Fuel Sci. Tech. Int. 10 (4-6) (1992) 723.
[28] L.C. Michon, D.A. Netzel, T.F. Turner, D. Martin, J.-P. Planche, Energy Fuel 13 (1999) 602.
[29] B. Wunderlich, Thermochim. Acta 300 (1997) 43.
[30] S. Paramanu, B.B. Pruden, P. Rahimi, Ind. Eng. Chem. Res. 38 (1999) 3121.
[31] H. Groenzin, O.C. Mullins, J. Phys. Chem. 103 (1999) 11237.
[32] A. Putnis, J.D.C. McConnell, Principles of Mineral Behaviour, Blackwell, Oxford, 1980, p. 145.
[33] E.P. Gilbert, Phys. Chem. Chem. Phys. 1 (1999) 1517.
[34] D.A. Anderson, M.O. Marasteanu, Transp. Res. Rec. 1661 (1999) 27.
[35] E.T. Samulski, The Mesomorphic State, in Physical Properties of Polymers, 2nd Edition, American Chemical Society, 1993, p. 201.
[36] J-F. Masson, G.M. Polomark, to be submitted.